JMEPEG (2011) 20:793–797
DOI: 10.1007/s11665-010-9751-9

1059-9495/$19.00

Rapid Obtaining of Nano-Hydroxyapatite Bioactive Films on NiTi Shape Memory Alloy by Electrodeposition Process

A.O. Lobo, J. Otubo, J.T. Matsushima, and E.J. Corat

(Submitted May 13, 2010; in revised form August 2, 2010)

Nano-hydroxyapatite (n-HA) crystalline films have been developed in this study by electrodeposition method on NiTi shape memory alloy (SMA). The electrodeposition of the n-HA films was carried out using 0.042 mol/L $Ca(NO_3)_2 \cdot 4H_2O$ + 0.025 mol/L $(NH_4) \cdot 2HPO_4$ electrolytes by applying a constant potential of −2.0 V for 120 min and keeping the solution temperature at 70 °C. The characterization of n-HA films is of special importance since bioactive properties related to n-HA have been directly identified with its specific composition and crystalline structure. AFM, XRD, EDX, FEG-SEM and Raman spectroscopy shows a homogeneous film, with high crystallinity, special composition, and bioactivity properties (Ca/P = 1.93) of n-HA on NiTi SMA surfaces. The n-HA coating with special structure would benefit the use of NiTi alloy in orthopedic applications.

Keywords crystallinity, electrodeposition, nano-hydroxyapatite, NiTi SMA

1. Introduction

NiTi shape memory alloys (SMAs) were introduced for biomedical applications in the late 1970s due to their unique shape memory, superelasticity, resistance to fatigue, and corrosion (Ref 1). Hydroxyapatite (HA) and other calcium phosphate coatings have been developed to increase the biocompatibility in orthopedic applications (Ref 2, 3). Such coatings promote the attachment of bone tissue and provide a mechanically stable interface between implant and bone (Ref 2, 3).

Many essential techniques have been used in the preparation of HA coatings, such as plasma spraying (Ref 4), magnetron sputtering (Ref 5), laser ablation (Ref 6), sol-gel (Ref 7), biomimetic (Ref 8), and electrochemical deposition (Ref 9). The most prominent problem of these techniques is, however, the interfacial adherence between the coating and the metal implant. In vivo tests of these coatings have shown lack of bonding strength to the metallic bio-inert substrate or re-absorption. These effects are mainly due to the presence of other calcium phosphate phases of poor stability in comparison with crystalline HA (Ref 10, 11).

The electrodeposition is an advantageous method for production of a thin, crystalline, homogeneous, and adherent film besides being an efficient, rapid, reproducible, and low-cost process (Ref 12). The composition and control of the coating structure are possible in part due to the relatively low processing temperature. The possibility of coating irregular surfaces is also of great importance. Hence, the electrodeposition of HA coating has attracted considerable attention in recent years.

Producing bioactive nano-HA (n-HA) coating on NiTi SMA combines the mechanical advantages of implant materials and biological affinity of the n-HA surface due to the similarity with natural bone tissue. The possibility of depositing it as film permits exploring its bioactive properties in structural prostheses.

This article shows for the first time the development of a method for obtaining rapidly the n-HA on NiTi SMA surfaces using the electrodeposition process. Crystallinity, reproducibility, stoichiometry, homogeneity, and biomineralization properties on NiTi alloy were observed.

2. Experimental Procedures

The starting material was a 150-mm diameter, 21-kg high purity NiTi ingot (Ti-55.3, Ni-0.016, and C-0.07 O in wt.%) produced by electron beam melting. The fabrication procedure

This article is an invited paper selected from presentations at Shape Memory and Superelastic Technologies 2010, held May 16-20, 2010, in Pacific Grove, California, and has been expanded from the original presentation.

A.O. Lobo and **E.J. Corat**, Instituto Tecnologico de Aeronautica, Praca Marechal Eduardo Gomes, 50, Vila das Acacias, CEP 12.228-900 São Jose dos Campos, SP, Brazil and Laboratorio Associado de Sensores e Materiais (LAS), Centro de Tecnologias Aeroespaciais (CTE), sala 20, Instituto Nacional de Pesquisas Espaciais, Avenida dos Astronautas 1758, Jardim da Granja, CEP 12.245-970 São Jose dos Campos, SP, Brazil; **J. Otubo**, Instituto Tecnologico de Aeronautica, Praca Marechal Eduardo Gomes, 50, Vila das Acacias, CEP 12.228-900 São Jose dos Campos, SP, Brazil and **J.T. Matsushima**, Laboratorio Associado de Sensores e Materiais (LAS), Centro de Tecnologias Aeroespaciais (CTE), sala 20, Instituto Nacional de Pesquisas Espaciais, Avenida dos Astronautas 1758, Jardim da Granja, CEP 12.245-970 São Jose dos Campos, SP, Brazil. Contact e-mails: loboao@yahoo.com and anderson@las.inpe.br.

can be seen elsewhere (Ref 13). A 7-mm-thick slice was taken from the ingot top position and hot rolled down to 1-mm-thick sheet, and then $10 \times 10 \times 1$ mm^3 samples were taken. Sample surfaces were polished with colloidal silica and then ultrasonically cleaned in acetone bath for 15 min. A supplementary preparation operation has been performed using an anodic electrolysis process (0.2 mol/L NaOH) with a current of 0.9 A for 10 min. The electrodeposition of the n-HA films on the NiTi SMA was performed using 0.042 mol/L $Ca(NO_3)_2 \cdot 4H_2O$ + 0.025 mol/L $(NH_4) \cdot 2HPO_4$ (pH = 4.7) electrolyte. The n-HA films were prepared by applying a constant potential of −2.0 V for 2 h with the solution temperature being kept at 70 °C. The electrochemical measurements were made using a three-electrode cell coupled to equipment (Autolab PGSTAT 302). NiTi SMA surfaces were used as working electrode, and the geometric area in contact with electrolytic solution was 0.27 cm^2. A platinum coil wire served as auxiliary electrode, and Ag/AgCl electrode was used as reference electrode. The n-HA film morphology structures were analyzed by a scanning electron microscopy (FEG-SEM, JEOL JSM-6330F). After deposition, all the specimens were rinsed with distilled water and ethanol, and then dried at 100 °C for 24 h. Atomic force microscopy (AFM, Veeco Multimode V) was used to characterize the average surface roughness of the n-HA coatings. The elemental composition (Ca, P, and O) of the n-HA coatings on the NiTi SMA surfaces was investigated by energy-dispersive x-ray analysis (EDX, JEOL-JSM-5310, Thermo Electro Corporation). Raman spectroscopy (Renishaw 2000) was used to determine the chemical composition of the n-HA films.

3. Results and Discussions

Figure 1 shows the evolution of current as function of the n-HA deposition time on NiTi SMA surfaces. Initially, a rapid increase of cathodic current due to the electric double-layer charging (region 1) was observed. The current continues to increase until it reaches a value of approximately 0.24 mA (region 2), which is associated to hydroxyl (OH^-) ion generation process due to the reduction of water and dissolved oxygen on non-uniform NiTi SMA surface. After approximately 10 min, the current decreases to a limit value, indicating that the OH^- ion generation process is limited by diffusion (region 3). In the electrochemical process, which involves the formation of n-HA, the OH^- ion generation on the surface is of interest for fundamental parameters that controls n-HA characteristics due to the acid-base reactions that form PO_4^{3-} and HPO_4^{2-} (Ref 9).

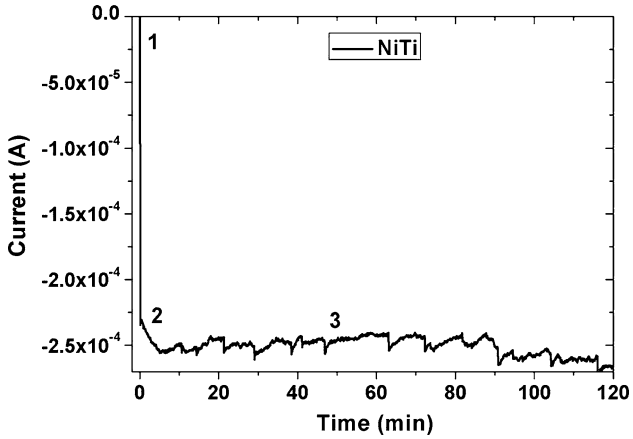

Fig. 1 Current-time profile during the deposition of n-HA films on NiTi SMA surface

Besides the surface chemistry, topography is another variable which strongly affects the process of electrodeposition. For instance, one might expect that the surface roughness generate charged regions, which are very susceptible to transfer electrons. Therefore, the structure of the coating would be significantly affected (Ref 14). In order to minimize this effect, it was decided to employ anodic electrolysis process on NiTi SMA surfaces instead of rough ones. Figure 2 shows the roughness of NiTi SMA surfaces before (a) and after (b) the n-HA electrodeposition. The surface roughness was measured over an area of 1×1 μm. Even though, all the NiTi SMA surfaces are considerably smooth (Ra ∼ 1 nm), one of the effects of the n-HA electrodeposition is the increase in the surface roughness (∼16.9 nm). The average grain size was approximately 100 nm after the n-HA electrodeposition.

Figure 3(a)-(c) shows FEG-SEM images of n-HA crystals formed on NiTi SMA surfaces. Figure 3(a) reveals a homogeneous layer of n-HA crystals formed on the NiTi SMA surfaces. Details of these observations are shown in Fig. 3(b). The coating surface exhibited different crystal characteristics and orientation. Lamellar, plate and needle-like crystal morphologies with no preferential orientations were observed (Fig. 3b).

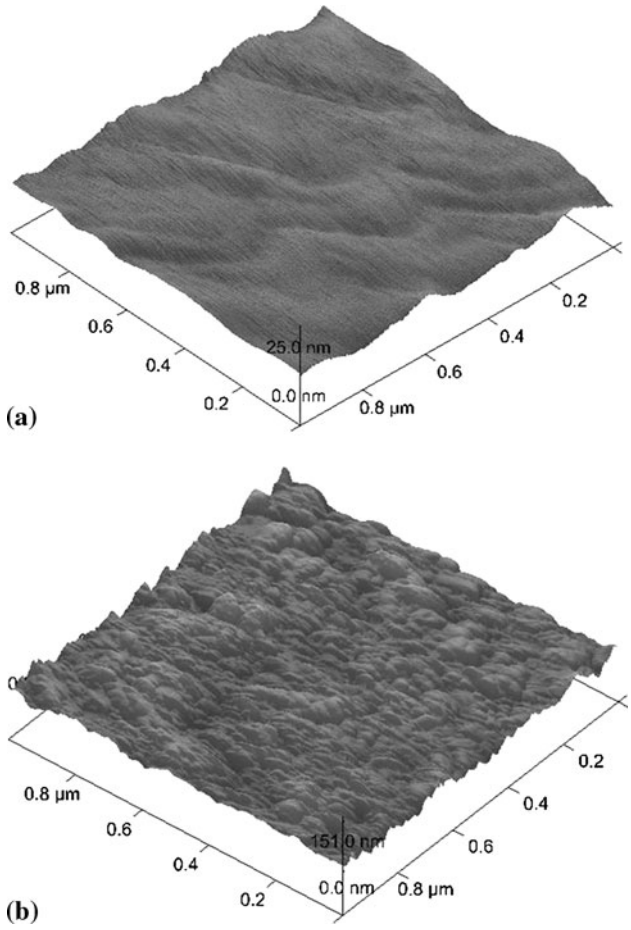

Fig. 2 3-D Atomic force microscopy images of (a) NiTi SMA surfaces and (b) grain of N-HA obtained after 3 h of electrodeposition at 70 °C

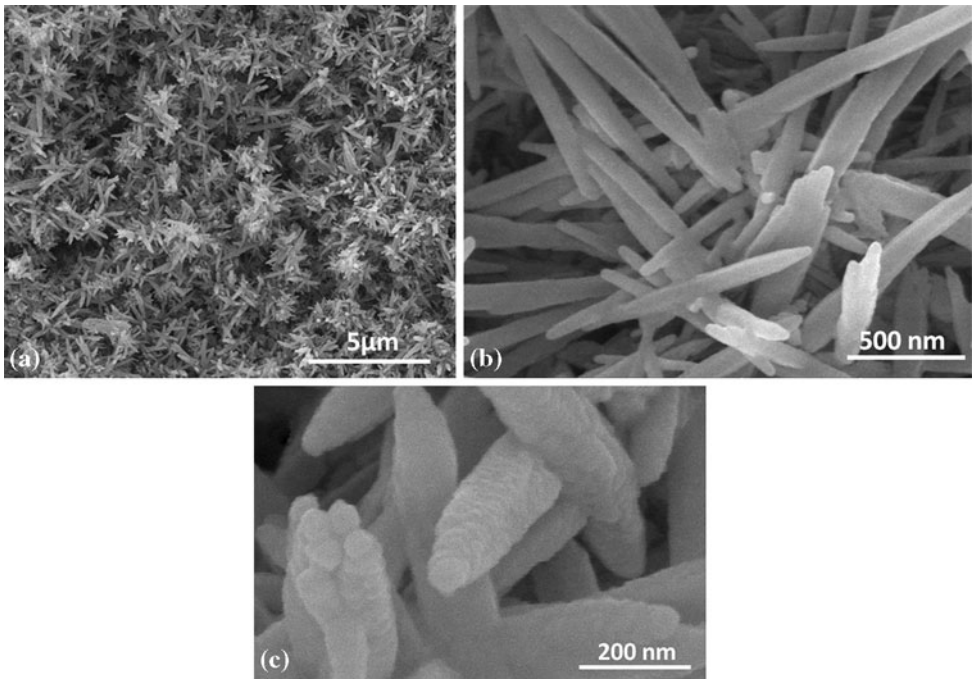

Fig. 3 Scanning electron microscopy images of n-HA on NiTi SMA surfaces. Composites obtained after 120 min of electrodeposition at 70 °C

Details of needle-like crystal morphologies (length of 1-3 μm and thickness of 60 nm) are shown with higher magnification in Fig. 3(c). The cortical bone tissue contains many different structures that exist on many levels of scale from 60 nm to 3000 μm (Ref 14). The dimensions of n-HA crystals presented in this article are similar to bone tissue. The results of FEG-SEM (Fig. 1) and AFM (Fig. 3) show that n-HA crystals are formed on NiTi SMA surfaces, suggesting an increase in the surface roughness with anodic electrolysis process, and a simple thermal treatment improving the nucleation and crystal growth of the n-HA.

It is well known (Ref 15) that substrate orientation is an important parameter that can define the crystallographic orientation of HA films, no matter which deposition technique is employed. It has also been proved that in certain conditions, the electrodeposition leads to a preferential orientation of crystals (Ref 16). Eliaz et al. have demonstrated that two distinct mechanisms may occur during HA electrodeposition on Ti6Al4V substrates, i.e. instantaneous and progressive nucleations (Ref 16). Those authors have assumed that the deposition process starts with a two-dimensional (2D) growth (progressive mechanism) and changes, after a few minutes, to a three-dimensional (3D) growth (instantaneous mechanism). Let us consider now the same hypothesis. After the anodic electrolysis process (base material), it would be the direct product of a 2D growth mechanism, whereas the formation of crystal clusters would be the result of the 3D growth mechanism (Fig. 3a-c). Santos et al. showed that the roughness control was necessary to obtain oriented and crystalline n-HA on Ti6Al4V alloy surfaces (Ref 17). However, the n-HA crystals presented here show different morphologies and orientation as can be seen in Fig. 3(b). These results suggest that further study related to control the anodic electrolysis process is necessary to obtain oriented n-HA crystals on NiTi SMA surfaces.

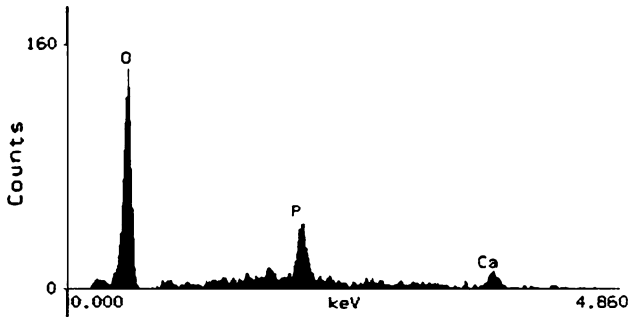

Fig. 4 Energy-dispersive x-ray spectrum of HA electrodeposited on NiTi SMA surfaces

The elemental composition of the coating was investigated by EDX analysis of the n-HA crystals grown on NiTi SMA surfaces (Fig. 4). The peak of Ca, P, and O shows the strong presence of n-HA coatings over the substrate. The Ca/P ratio determined from the analysis was 1.93, which is higher than the stoichiometric HA (1.67) presented by bone tissue (Ref 18).

A comparison between x-ray diffraction (XRD, X-Pert Philips) of NiTi SMA surfaces (a) and n-HA growth on NiTi SMA surfaces (b) is shown in Fig. 5. Diffraction peaks of NiTi SMA surfaces were observed in both diffractograms. Notice that, the apatite formation is highlighted due to the presence of several characteristic x-ray reflection peaks in the diffraction pattern shown in Fig. 5(b). It can be seen that the peaks at 2-theta of 25.9°, 31.7°, 32.9°, and 39.8° are assigned to (002), (211), (300), and (310) lattice planes of n-HA, respectively (Ref 19). Ozeki et al. suggested that the preferential growth of HA in (001) direction due to the *c*-axis in HA is shorter than that due to the *a*-axis (Ref 20). Onuma et al. described the preferential HA growth in (001) direction with cluster growth

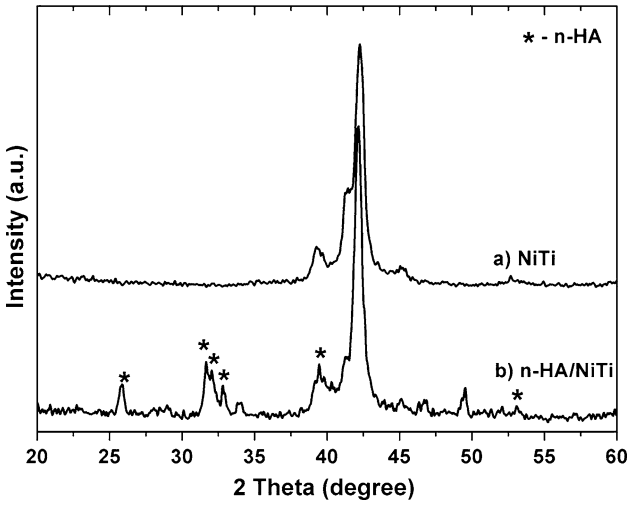

Fig. 5 X-ray diffractograms of NiTi SMA surfaces before (a) and after (b) the n-HA electrodeposition

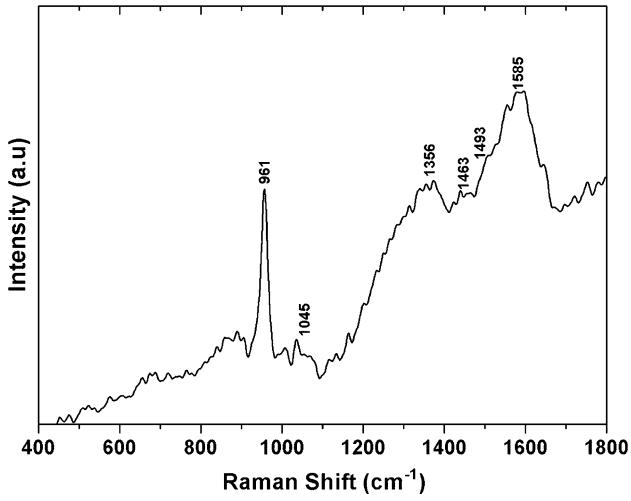

Fig. 6 Raman spectrum of the n-HA electrodeposited on NiTi SMA surfaces

model, where $Ca_9(PO_4)_6$ clusters are situated along the *c*-axis (Ref 21). This observation corroborates the finding of n-HA crystal presence strongly oriented along the *c*-axis.

Raman spectroscopy can be considered as a fast method for analyzing molecular properties of bulk, interfaces and surfaces of HA. A typical Raman spectrum of n-HA on NiTi SMA surface is shown in Fig. 6. This figure shows the phosphate vibration mode region, and a particular attention is drawn to the most intense non-degenerated vibration mode ν_1 near 960 cm^{-1}, corresponding to the symmetric stretching of P-O bonds, characteristic of HA layer. Raman spectra show symmetric stretching vibrations of carboxylate groups (C-O) that are assigned to the peaks at 1356, 1463, 1483, 1463, and 1356 cm^{-1}. The P-O stretching observed in Raman band recorded at 1040-1045 cm^{-1} is similar to a human bone ex vivo formed (Ref 22). A broad band at $\sim$1600 cm^{-1} is also observed, which can be attributed to the presence of carbonate at channel sites (Ref 22).

Bone growth at the implant surface requires the presence of sufficient amount of calcium and phosphate ions and local supersaturation of body fluid which is a necessary condition for increasing bone growth (Ref 23). Apatite deposition on NiTi SMA surfaces has been reported by Yang's group in a number of manuscripts using other methods (Ref 24, 25). In these studies, pre-treatment of surfaces with NaOH using HNO_3 followed by NaOH was carried out before soaking in a Ca-P solution (Ref 24). Chen et al. showed that Ti-OH groups formed with an acid treatment are sufficient to increase apatite formation from SBF solution after 1 day on NiTi SMA surfaces (Ref 25), because Ti-OH groups play a role in absorbing Ca^{2+} and PO_4 ions in SBF. Liu et al. showed that an oxidation to produce Al_2O_3 on NiTi alloy surface was necessary for apatite formation after 14 days' soaking in SBF (Ref 26). The Ca/P ratio presented by these authors was about 1.62. Owing to the difference in the pre-treatment and also in the calcification treatment, the Ca/P ratio presented in this study is different from those ones (Ca/P = 1.93). The results of this study show that NiTi SMA surfaces were efficient for the growth of n-HA using an electrodeposition process. These results show that NiTi SMA surfaces after the anodic electrolysis process were able to nucleate n-HA crystals for electrodeposition in basic conditions. This result also proved that control of the initial stage is essential to obtain n-HA nucleation with higher crystallinity.

4. Conclusion

In summary, the results of this study showed that NiTi SMA was efficient for the growth of n-HA using an electrodeposition process. The high mineralization (Ca/P = 1.93) and the presence of homogeneous n-HA crystals can be achieved after 2 h. These results are important to accelerate the biomimetic mineralization because the design and composition of NiTi/n-HA alloys obtained in this study will be used as precursor for nucleation sites for in vitro or in vivo HA depositions. Further investigations of tribology and biocompatibilility (in vitro and in vivo) will be required for assessing their possibility for applications in orthopedic implants.

Acknowledgments

We gratefully acknowledge funding by Fundacao de Amparo a Pesquisa do Estado de Sao Paulo under the Grants 08/116425 and 07/00013-4, to FINEP grant PROINFRA 01/05/153), CNPq (grants 473612/2006-2 and 620091/2008-8) and to AEB (grant 010-460000).

References

1. A. Kapanen, J. Ryhanen, and A. Danilov, Effect of Nickel-Titanium Shape Memory Metal Alloy on Bone Formation, *Biomaterials*, 2001, **22**, p 2475–2480
2. X.J. Yang, R.X. Hu, S.L. Zhu, C.Y. Li, M.F. Chen, L.Y. Zhang, and Z.D. Cui, Accelerating the Formation of a Calcium Phosphate Layer on NiTi Alloy by Chemical Treatments, *Scr. Mater.*, 2006, **54**, p 1457–1462
3. P. Filip, A.C. Kneissl, and K. Mazanec, Physics of Hydroxyapatite Plasma Coatings on TiNi Shape Memory Materials, *Mater. Sci. Eng. A*, 1997, **234**, p 422–425

4. J.L. Ong and D.C.N. Chan, Hydroxyapatite and Their Use as Coatings in Dental Implants: A Review, *Crit. Rev. Biomed. Eng.*, 1999, **28**, p 667–707
5. S. Ding, Properties and Immersion Behavior of Magnetron-Sputtered Multi-Layered Hydroxyapatite/Titanium Composite Coatings, *Biomaterials*, 2003, **24**, p 4233–4238
6. J.G.C. Wolke, J.P.C.M. Van Der Waerden, H.G. Schaeken, and J.A. Jansen, In Vivo Dissolution Behavior of Various RF Magnetron-Sputtered Ca-P Coatings on Roughened Titanium Implants, *Biomaterials*, 2003, **24**, p 2623–2629
7. D. Liu, Q. Yang, and T. Troczynski, Sol-Gel Hydroxyapatite Coatings on Stainless Steel Substrates, *Biomaterials*, 2002, **23**, p 691–698
8. X.X. Wang, L. Xie, and R.Z. Wang, Biological Fabrication of Nacreous Coating on Titanium Dental Implant, *Biomaterials*, 2005, **26**, p 6229–6232
9. J. Ma, C. Wang, and K.W. Peng, Electrophoretic Deposition of Porous Hydroxyapatite Scaffold, *Biomaterials*, 2003, **24**, p 3505–3510
10. G.L. Lange and K. Donath, Interface Between Bone Tissue and Implants of Solid Hydroxyapatite or Hydroxyapatite-Coated Titanium Implants, *Biomaterials*, 1989, **10**(10), p 121–125
11. S.R. Sousa and M.A. Barbosa, Effect of Hydroxyapatite Thickness on Metal Ion Release From Ti6Al4V Substrates, *Biomaterials*, 1996, **17**, p 397–404
12. M. Manso, C. Jiménez, C. Morant, P. Herrero, and J.M. Martínez-Duart, Electrodeposition of Hydroxyapatite Coatings in Basic Conditions, *Biomaterials*, 2000, **21**(17), p 1755–1761
13. J. Otubo and A.S. Antunes, Characterization of 150 mm in Diameter NiTi SMA Ingot Produced by Electron Beam Melting, *Mater. Sci. Forum*, 2010, **643**, p 55–59
14. T.J. Webster, M.C. Waid, J.L. McKenzie, R.L. Price, and J.U. Ejiofor, Nano-Biotechnology: Carbon Nanofibres as Improved Neural and Orthopaedic Implants, *Nanotechnology*, 2004, **15**, p 48–54
15. Z.D. Hong, L. Luan, S.B. Paik, B. Deng, D.E. Ellis, J.B. Ketterson et al., Crystalline Hydroxyapatite Thin Films Produced at Room Temperature—An Opposing Radio Frequency Magnetron Sputtering Approach, *Thin Solid Films*, 2007, **515**, p 6773–6780
16. N. Eliaz and M. Eliyahu, Electrochemical Processes of Nucleation and Growth of Hydroxyapatite on Titanium Supported by Real-Time Electrochemical Atomic Force Microscopy, *J. Biomed. Mater. Res. A*, 2007, **80A**, p 621–634
17. E.A. dos Santos, M.S. Moldovan, L. Jacomine, M. Mateescu, J. Werckmann, K. Anselme et al., Oriented Hydroxyapatite Single Crystals Produced by the Electrodeposition Method, *Mater. Sci. Eng. B*, 2010, **169**, p 138–144
18. S. Kale, S. Biermann, C. Edwards, C. Tarnowski, M. Morris, and M.W. Long, Three-Dimensional Cellular Development is Essential for the Ex Vivo Formation of Human Bone, *Nat. Biotechnol.*, 2000, **18**, p 954–958
19. H.P. Klug and L.E. Alexander, *X-ray Diffraction Procedures*, John Wiley, New York, 1954
20. K. Ozeki, H. Aoki, and Y. Fukui, Effect of pH on Crystallization of Sputtered Hydroxyapatite Film Under Hydrothermal Conditions at Low Temperature, *J. Mater. Sci.*, 2005, **40**, p 2837–2842
21. K. Onuma and A. Ito, Cluster Growth Model for Hydroxyapatite, *Chem. Mater.*, 1998, **10**, p 3346–3351
22. J. Mahamid, A. Sharir, L. Addadi, and S. Weiner, Amorphous Calcium Phosphate is a Major Component of the Forming Fin Bones of Zebrafish: Indications for an Amorphous Precursor Phase, *PNAS*, 2008, **105**, p 12748–12753
23. X. Lu, Z. Zhao, and Y. Leng, Calcium Phosphate Crystal Growth Under Controlled Atmosphere in Electrochemical Deposition, *J Cryst. Growth*, 2005, **284**, p 506–516
24. M.F. Chen, X.J. Yang, R.X. Hu, Z.D. Cui, and H.C. Man, Bioactive NiTi Shape Memory Alloy Used as Bone Bonding Implants, *Mater. Sci. Eng. C Biomim. Mater. Sens. Syst.*, 2004, **4**, p 497–502
25. M.F. Chen, X.J. Yang, Y. Liu, S.L. Zhu, Z.D. Cui, and H.C. Man, Study on the Formation of an Apatite Layer on NiTi Shape Memory Alloy Using a Chemical Treatment Method, *Surf. Coat. Technol.*, 2003, **173**, p 229–234
26. F. Liu, J. Xu, F. Wang, L. Zhao, and T. Shimizu, Biomimetic Deposition of Apatite Coatings on Micro-Arc Oxidation Treated Biomedical NiTi Alloy, *Surf. Coat. Technol.*, 2010, **204**(20), p 3294–3299